Available online at www.sciencedirect.com
SCIENCE DIRECT®
Applied Thermal Engineering 25 (2005) 2478–2495
APPLIED THERMAL ENGINEERING
www.elsevier.com/locate/apthermeng

A transient 3-D inverse problem in imaging the time-dependent local heat transfer coefficients for plate fin

Cheng-Hung Huang *, Yao-Long Tsai

Department of Systems and Naval Mechatronic Engineering, National Cheng Kung University, Tainan 701, Taiwan, ROC

Received 18 August 2004; accepted 5 December 2004
Available online 11 February 2005

Abstract

The local time-dependent surface heat transfer coefficients for plate finned-tube heat exchangers are estimated in a three-dimensional inverse heat conduction problem. The inverse algorithm utilizing the steepest descent method (SDM) and a general purpose commercial code CFX4.4 is applied successfully in this study in accordance with the simulated measured temperature distributions on fin surface by infrared thermography. Two different heat transfer coefficients for staggered as well as in-line tube arrangements with different measurement errors are determined. Results of the numerical simulation show that the reliable estimated heat transfer coefficients can be obtained by using the present inverse algorithm.

Keywords: Inverse problem; Heat transfer coefficient estimation; Plate fin

1. Introduction

Heat exchangers are the workhorse of industry. Variously known as condensers, coolers, evaporators, heaters, vaporizers, and so forth. Finned surfaces of the plate finned-tube heat exchangers have been in use over a long period of time for dissipation of heat by convection. Applications for finned surfaces are widely seen in air-conditioning, electrical, chemical, refrigeration, cryogenics

* Corresponding author. Tel.: +886 6 274 7018; fax: +886 6 274 7019.
E-mail address: chhuang@mail.ncku.edu.tw (C.-H. Huang).

1359-4311/$ - see front matter
doi:10.1016/j.applthermaleng.2004.12.003

Nomenclature

$J[h(S_i,t)]$ functional defined by Eq. (3)
$J'[h(S_i,t)]$ gradient of functional defined by Eq. (15)
k thermal conductivity
$P^n(S_i,t)$ direction of descent defined by Eq. (5)
$T(\Omega,t)$ estimated temperature
$\Delta T(\Omega,t)$ sensitivity function defined by Eq. (6)
$Y(S_i,t)$ measured temperature

Greek symbols
β search step size
$\lambda(\Omega,t)$ Lagrange multiplier defined by Eq. (12)
ε convergence criteria

Superscripts
n iteration index
$\hat{}$ estimated value

and many cooling systems in industrial. Kays and London [1] introduced various types of heat transfer surfaces.

With the current awareness and concern about energy and resource conservation as well as efficient operation of plants, it is imperative that the heat exchangers be designed and operated optimally. To achieve this goal the estimation of local convective heat transfer coefficients for fin surface becomes very important in designing the high-performance heat exchangers. Unfortunately, the estimation of the convective heat transfer coefficient is more difficult to perform than other common thermo-fluid-dynamic quantities, especially in case of non-uniform distributions and/or of conduction–convection problem.

Ay et al. [2] applied a control volume based finite difference formulation and an infrared thermography based temperature measurements to estimate the local heat transfer coefficients of plate fin in a 2-D inverse heat conduction problem. Recently, Huang et al. [3] used the technique of steepest descent method (SDM) and commercial code CFX4.4 [4] to estimate the local convective heat transfer coefficients over fin surface in a steady-state 3-D inverse heat conduction problem based on the simulated temperature measurements by infrared thermography. The steepest descent method has great potential in solving the 3-D inverse problem. However the 3-D inverse heat conduction problem in estimating the time-dependent local convective heat transfer coefficients on fin surface has never been examined.

The technique of utilizing the inverse algorithms together with the commercial code CFX4.2 has been developed successfully by Huang and Wang [5], they applied the algorithm to estimate the unknown surface heat fluxes in a 3-D solid. By following similar technique, Huang and Chen [6] estimated successfully the unknown boundary heat flux in a 3-D inverse heat convection problem. Huang and Cheng [7] estimated the heat generation rate of chips on a PC board. More

recently, Huang and Li [8] applied the algorithm to an optimal heating problem in determining the optimal surface heat fluxes for a three-dimensional forced convection problem.

It should be noted that all of the above applications are 3-D inverse problems, this implies that the algorithm is powerful since the 3-D inverse problems are still very limited in the open literature.

The present iterative algorithm can also be found in many works. For instance, Loulou and Artioukhine [9] determined the optimal choice of vectorial descent parameter for used in the iterative regularization method and showed a considerable increase in the convergence rate. Louahlia-Gualous et al. [10] determined the local heat transfer for nucleate pool boiling around the cylinder using the iterative regularization method. Loulou and Scott [11] used an iterative regularization method to a 3-D heat flux from surface temperature measurements.

The objective of this study is to extend a 3-D steady-state inverse problem [3] to a transient 3-D inverse problem in estimating the time-dependent local convective heat transfer coefficients of finned surfaces for the plate finned-tube heat exchangers. The number of unknown heat transfer coefficients will increase tremendously under present consideration and this will also increase the difficulty in solving the present inverse problem.

The steepest descent method derives basis from the perturbational principle [12] and transforms the inverse problem to the solution of three problems, namely, the direct problem, the sensitivity problem and the adjoint problem, which will be discussed in detail in the text.

2. Direct problem

A typical plate finned-tube heat exchanger is shown in Fig. 1. The plate fins of staggered and in-line arrangements with domain $\Omega(x, y, z)$ are illustrated in Fig. 2a and b, respectively. The grid

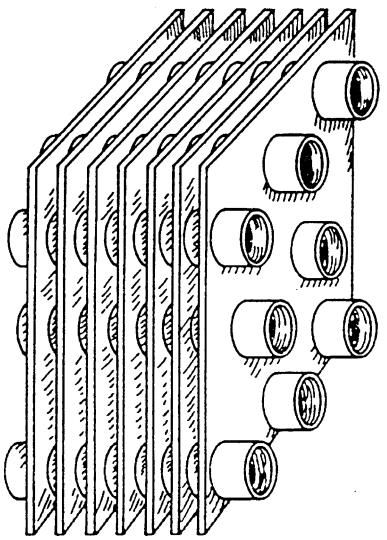

Fig. 1. A typical plate finned-tube heat exchanger.

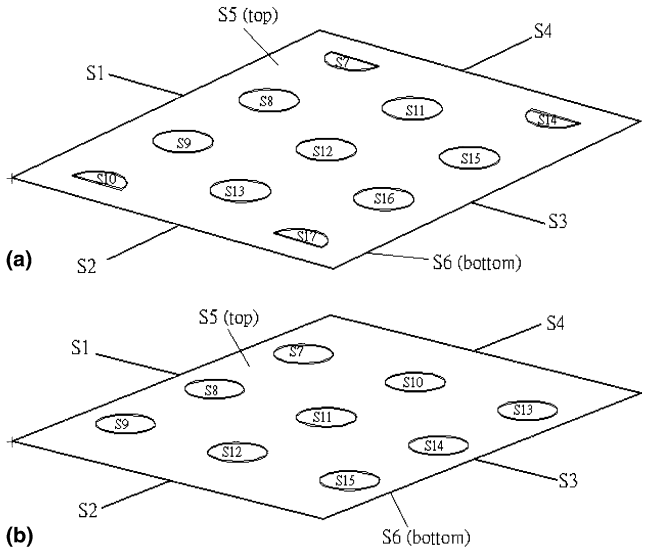

Fig. 2. (a) The geometry of plate fin in staggered arrangement for use in test case 1. (b) The geometry of plate fin in in-line arrangement for use in test case 2.

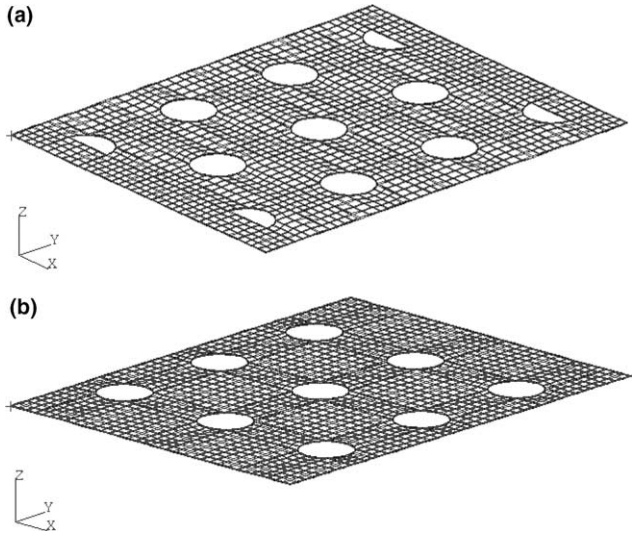

Fig. 3. (a) The grid system for staggered arrangement for use in test case 1. (b) The grid system for in-line arrangement for use in test case 2.

system used in numerical experiments for both arrangements are shown in Fig. 3a and b, respectively. The surface on S_i, $i = 1$–6, are subjected to a convective boundary condition with prescribed heat transfer coefficient $h(S_i, t)$, $i = 1$–6, where $i = 1$–4 represent the edge boundaries; while $i = 5$ and 6 indicate the top and bottom surfaces, respectively. The unknown heat transfer coefficient $h(S_i, t)$ could be function of temperature in the present study. The tube boundary

surfaces on S_i, $i = 7$ to $(I + 6)$, are subjected to a prescribed temperature condition $T = T(S_i, t)$, where I represents the number of tube.

The formulation of this three-dimensional transient heat conduction problem can be expressed as:

$$k\left[\frac{\partial^2 T(\Omega,t)}{\partial x^2}+\frac{\partial^2 T(\Omega,t)}{\partial y^2}+\frac{\partial^2 T(\Omega,t)}{\partial z^2}\right]=\rho Cp\frac{\partial T(\Omega,t)}{\partial t} \quad \text{in}(\Omega,t) \tag{1a}$$

$$-k\frac{\partial T(S_1,t)}{\partial x}=h(S_1,t)(T_\infty-T) \quad \text{on fin surface } S_1 \tag{1b}$$

$$-k\frac{\partial T(S_2,t)}{\partial x}=h(S_2,t)(T-T_\infty) \quad \text{on fin surface } S_2 \tag{1c}$$

$$-k\frac{\partial T(S_3,t)}{\partial y}=h(S_3,t)(T_\infty-T) \quad \text{on fin surface } S_3 \tag{1d}$$

$$-k\frac{\partial T(S_4,t)}{\partial y}=h(S_4,t)(T-T_\infty) \quad \text{on fin surface } S_4 \tag{1e}$$

$$-k\frac{\partial T(S_5,t)}{\partial z}=h(S_5,t)(T_\infty-T) \quad \text{on fin surface } S_5 \tag{1f}$$

$$-k\frac{\partial T(S_6,t)}{\partial z}=h(S_6,t)(T-T_\infty) \quad \text{on fin surface } S_6 \tag{1g}$$

$$T=T(S_i,t) \quad \text{on tube surfaces, } i=7 \text{ to } I+6 \tag{1h}$$

$$T=T_\infty(\Omega,t) \quad \text{for } t=0 \tag{1i}$$

Here k is the thermal conductivity of fin, ρ and Cp are the density and heat capacity of the material, respectively.

The edge surface area S_i, $i = 1$–4 is small enough when comparing with top and bottom surfaces S_i, $i = 5$–6. This implies that the heat transfer rate through S_i, $i = 1$–4 can be neglected. For this reason we assume that the boundary conditions on surface S_i, $i = 1$–4 are adiabatic conditions. Meanwhile, the fin thickness is being thin, the temperature distribution on S_5 should be very close to S_6 for any time t, therefore it is also reasonable to assume that the heat transfer coefficients on S_5 and S_6 are equal to each other, i.e. $h(S_5, t) = h(S_6, t)$. The direct problem becomes

$$k\left[\frac{\partial^2 T(\Omega,t)}{\partial x^2}+\frac{\partial^2 T(\Omega,t)}{\partial y^2}+\frac{\partial^2 T(\Omega,t)}{\partial z^2}\right]=\rho Cp\frac{\partial T(\Omega,t)}{\partial t} \quad \text{in } \Omega(x,y,z,t) \tag{2a}$$

$$\frac{\partial T(S_i,t)}{\partial n}=0 \quad \text{on fin surface } S_i,\ i=1\text{–}4 \tag{2b}$$

$$-k\frac{\partial T(S_5,t)}{\partial z}=h(S_5,t)(T_\infty-T) \quad \text{on fin surface } S_5 \tag{2c}$$

$$-k\frac{\partial T(S_6,t)}{\partial z} = h(S_6,t)(T - T_\infty) \quad \text{on fin surface } S_6 \tag{2d}$$

$$T(S_i,t) = T_0 \quad \text{on tube surfaces, } i = 7 \text{ to } I+6 \tag{2e}$$

$$T(\Omega,t) = T_\infty \quad \text{for } t = 0 \tag{2f}$$

The direct problem considered here is concerned with calculating the plate fin temperatures when the heat transfer coefficient $h(S_i,t)$, $i = 5$ and 6, thermal properties as well as the initial and boundary conditions on tube surfaces are known. The solution for the above 3-D heat conduction problem in domain Ω is solved using CFX4.4 and its Fortran subroutine USRBCS.

3. The inverse problem

For the inverse problem considered here, the local time-dependent heat transfer coefficients $h(S_i,t)$, $i = 5$ and 6, are regarded as being unknown, but everything else in Eq. (2) is known. In addition, the simulated temperature readings using infrared thermography on the fin surface S_5 and S_6 are assume available.

Let the temperature reading taken by infrared scanners on fin surfaces S_5 and S_6 be denoted by $Y(S_i,t) \equiv Y(x_m,y_m,t) \equiv Y_m(S_i,t)$, $m = 1$ to M and $i = 5$ and 6, where M represents the number of measured temperature extracting points. This inverse problem can be stated as follows: by utilizing above mentioned measured temperature data $Y_m(S_i,t)$, estimate the unknown local time-dependent heat transfer coefficients $h(S_i,t)$.

The solution of this inverse problem is to be obtained in such a way that the following functional is minimized:

$$J[h(S_i,t)] = \int_{t=0}^{t_f}\sum_{m=1}^{M}[T_m(S_i,t) - Y_m(S_i,t)]^2\,\mathrm{d}t \quad i = 5 \text{ and } 6 \tag{3}$$

here, $T_m(S_i,t)$ are the estimated or computed temperatures at the measured temperature extracting locations (x_m,y_m) and time t. These quantities are determined from the solution of the direct problem given previously by using the estimated local heat transfer coefficients $h(S_i,t)$.

4. Steepest descent method for minimization

An iterative process based on the steepest descent method [12] is now applied for the estimation of unknown heat transfer coefficients $h(S_i)$ by minimizing the functional $J[h(S_i,t)]$

$$h^{n+1}(S_i,t) = h^n(S_i,t) - \beta^n P^n(S_i,t) \quad \text{for } n = 0,1,2,\ldots \quad \text{and} \quad i = 5,6 \tag{4}$$

where β^n is the search step size in going from iteration n to iteration $n+1$, and $P^n(S_i,t)$ is the direction of descent (i.e. search direction) given by

$$P^n(S_i,t) = J'^n(S_i,t) \quad i = 5 \text{ and } 6 \tag{5}$$

which is the gradient direction $J'^n(S_i,t)$ at iteration n.

To complete the iterations in accordance with Eq. (4), the step size β^n and the gradient of the functional $J'^n(S_i,t)$ need be computed. In order to develop expressions in determining these two quantities, a "sensitivity problem" and an "adjoint problem" need be constructed as described below.

4.1. Sensitivity problem and search step size

It is assumed that when $h(S_i,t)$ undergoes a variation Δh, T is perturbed by $T+\Delta T$. Then replacing in the direct problem h by $h+\Delta h$ and T by $T+\Delta T$, subtracting from the resulting expressions the direct problem and neglecting the second-order terms, the following sensitivity problem for the sensitivity function ΔT are obtained.

$$k\left[\frac{\partial^2\Delta T(\Omega,t)}{\partial x^2}+\frac{\partial^2\Delta T(\Omega,t)}{\partial y^2}+\frac{\partial^2\Delta T(\Omega,t)}{\partial z^2}\right]=\rho Cp\frac{\partial\Delta T(\Omega,t)}{\partial t}\quad\text{in }\Omega(x,y,z,t) \tag{6a}$$

$$\frac{\partial\Delta T(S_i,t)}{\partial n}=0\quad\text{on fin surfaces } S_i,\ i=1\text{–}4 \tag{6b}$$

$$-h(S_5,t)\Delta T+k\frac{\partial\Delta T}{\partial z}=\Delta h(S_5,t)(T-T_\infty)\quad\text{on fin surface } S_5 \tag{6c}$$

$$h(S_6,t)\Delta T+k\frac{\partial\Delta T}{\partial z}=\Delta h(S_6,t)(T_\infty-T)\quad\text{on fin surface } S_6 \tag{6d}$$

$$\Delta T(S_i,t)=0\quad\text{on tube surfaces, } i=7\text{ to }I+6 \tag{6e}$$

$$\Delta T(\Omega,t)=0\quad\text{for } t=0 \tag{6f}$$

CFX4.4 is used to solve the above sensitivity problem.

The functional $J[h^{n+1}(S_i,t)]$ for iteration $n+1$ is obtained by rewriting Eq. (3) as

$$J[h^{n+1}(S_i,t)]=\int_{t=0}^{t_f}\sum_{m=1}^{M}[T_m(S_i,t;h^n-\beta^nP^n)-Y_m(S_i,t)]^2\,\mathrm{d}t\quad i=5\text{ and }6 \tag{7}$$

where we replaced h^{n+1} by the expression given by Eq. (4). If temperature $T_m(S_i,t;h^n-\beta^nP^n)$ is linearized by a Taylor expansion, Eq. (7) takes the form

$$J[h^{n+1}(S_i,t)]=\int_{t=0}^{t_f}\sum_{m=1}^{M}[T_m(S_i,t;h^n)-\beta^n\Delta T_m(S_i,t;P^n)-Y_m(S_i,t)]^2\,\mathrm{d}t\quad i=5\text{ and }6 \tag{8}$$

where $T_m(S_i,t;h^n)$ is the solution of the direct problem by using the estimate heat transfer coefficients for the exact heat transfer coefficients on S_i, $i=5$ and 6. The sensitivity functions $\Delta T_m(S_i,t;P^n)$ are taken as the solutions of problem (6) at the measured temperature extracting positions (x_m,y_m,z_m,t) by using $\Delta h=P^n$. The search step size β^n is determined by minimizing the functional given by Eq. (8) with respect to β^n. The following expression results:

$$\beta^n=\frac{\int_{t=0}^{t_f}\sum_{m=1}^{M}[T_m(S_i,t)-Y_m(S_i,t)]\Delta T_m(S_i,t)\,\mathrm{d}t}{\int_{t=0}^{t_f}\sum_{m=1}^{M}[\Delta T_m(S_i,t)]^2\,\mathrm{d}t}\quad i=5\text{ and }6 \tag{9}$$

4.2. Adjoint problem and gradient equation

To obtain the adjoint problem, Eq. (2a) is multiplied by the Lagrange multiplier (or adjoint function) $\lambda(\Omega,t)$ and the resulting expression is integrated over the correspondent space domain. Then the result is added to the right hand side of Eq. (3) to yield the following expression for the functional $J[h(S_i,t)]$:

$$\begin{aligned} J[h(S_i,t)] &= \int_{t=0}^{t_f}\sum_{m=1}^{M}[T_m(S_i,t)-Y_m(S_i,t)]^2\,\mathrm{d}t \\ &\quad+\int_{t=0}^{t_f}\int_{\Omega}\left[\lambda(\Omega,t)\times\left(\nabla^2T-\rho Cp\frac{\partial T}{\partial t}\right)\right]\mathrm{d}\Omega\,\mathrm{d}t \\ &=\int_{t=0}^{t_f}\int_{S_i}[T(S_i,t)-Y(S_i,t)]^2\delta(x-x_m)\delta(y-y_m)\,\mathrm{d}S_i\,\mathrm{d}t \\ &\quad+\int_{t=0}^{t_f}\int_{\Omega}\left[\lambda(\Omega,t)\times\left(\nabla^2T-\rho Cp\frac{\partial T}{\partial t}\right)\right]\mathrm{d}\Omega\,\mathrm{d}t \quad \text{in } (\Omega,t),\ i=5 \text{ and } 6 \end{aligned} \tag{10}$$

where $\delta(\bullet)$ is the Dirac delta function and $(x_m,y_m,t), m = 1\text{–}M$, refers to the measured temperature extracting positions.

The variation ΔJ can be obtained by perturbing h by Δh and T by ΔT in Eq. (10), subtracting from the resulting expression the original equation (10) and neglecting the second-order terms. We thus find

$$\begin{aligned} \Delta J[h(S_i,t)] &= \int_{t=0}^{t_f}\int_{S_i}2[T(S_i,t)-Y(S_i,t)]\,\Delta T(S_i,t)\delta(x-x_m)\delta(y-y_m)\,\mathrm{d}S_i\,\mathrm{d}t \\ &\quad+\int_{t=0}^{t_f}\int_{\Omega}\left[\lambda(\Omega,t)\times\left(\nabla^2\Delta T-\rho Cp\frac{\partial\,\Delta T}{\partial t}\right)\right]\mathrm{d}\Omega\,\mathrm{d}t \quad \text{in } (\Omega,t),\ i=5 \text{ and } 6 \end{aligned} \tag{11}$$

In Eq. (11), the domain integral term is reformulated based on the Green's second identity; the boundary conditions of the sensitivity problem given by Eqs. 6(b)–6(e) are utilized and then ΔJ is allowed to go to zero. The vanishing of the integrands containing ΔT leads to the following adjoint problem for the determination of $\lambda(\Omega,t)$:

$$k\left[\frac{\partial^2\lambda(\Omega,t)}{\partial x^2}+\frac{\partial^2\lambda(\Omega,t)}{\partial y^2}+\frac{\partial^2\lambda(\Omega,t)}{\partial z^2}\right]+\rho Cp\frac{\partial\lambda(\Omega,t)}{\partial t}=0 \quad \text{in } (\Omega,t) \tag{12a}$$

$$\frac{\partial\lambda(\Omega,t)}{\partial n}=0 \quad \text{on fin surfaces } S_i,\ i=1\text{–}4 \tag{12b}$$

$$-\lambda h+k\frac{\partial\lambda}{\partial n}=2k[T(S_5,t)-Y(S_5,t)]\delta(x-x_m)\delta(y-y_m) \quad \text{on fin surface } S_5 \tag{12c}$$

$$\lambda h+k\frac{\partial\lambda}{\partial n}=2k[T(S_6,t)-Y(S_6,t)]\delta(x-x_m)\delta(y-y_m) \quad \text{on fin surface } S_6 \tag{12d}$$

$$\lambda(S_i,t)=0 \quad \text{on tube surfaces, } i=7 \text{ to } I+6 \tag{12e}$$

$$\lambda(\Omega,t)=0 \quad \text{for } t=t_f \tag{12f}$$

Finally, the following integral term is left

$$\Delta J=\int_{t=0}^{t_f}\int_{S_5}\frac{\lambda(S_5,t)}{k}[T(S_5,t)-T_\infty]\,\Delta h(S_5,t)\,\mathrm{d}S_5\,\mathrm{d}t - \int_{t=0}^{t_f}\int_{S_6}\frac{\lambda(S_6,t)}{k}[T(S_6,t)-T_\infty]\,\Delta h(S_6,t)\,\mathrm{d}S_6\,\mathrm{d}t \tag{13}$$

From definition [9], the functional increment can be presented as

$$\Delta J=\int_{t=0}^{t_f}\int_{S_5}J'(S_5,t)\,\Delta h(S_5,t)\,\mathrm{d}S_5\,\mathrm{d}t-\int_{t=0}^{t_f}\int_{S_6}J'(S_6,t)\,\Delta h(S_6,t)\,\mathrm{d}S_6\,\mathrm{d}t \tag{14}$$

A comparison of Eqs. (13) and (14) leads to the following expression for the gradient of the functional $J[h(S_i,t]$:

$$J'[h(S_i,t)]=\frac{\lambda(S_i,t)}{k}[T(S_i,t)-T_\infty] \quad \text{on surfaces } S_i,\ i=5 \text{ and } 6 \tag{15}$$

4.3. Stopping criterion

If the problem contains no measurement errors, the traditional check condition is specified as

$$J[h^{n+1}(S_i,t)]<\varepsilon \quad i=5 \text{ and } 6 \tag{16}$$

where ε is a small-specified number. However, the observed temperature data may contain measurement errors. Therefore, we do not expect the functional equation (3) to be equal to zero at the final iteration step. Following the experiences of the authors [5–8], we used the discrepancy principle as the stopping criterion, i.e. we assume that the temperature residuals may be approximated by

$$T_m(S_i,t)-Y_m(S_i,t)\approx\sigma \quad i=5 \text{ and } 6 \tag{17}$$

where σ is the standard deviation of the measurements, which is assumed to be a constant. Substituting Eq. (17) into Eq. (3), the following expression is obtained for stopping criteria ε:

$$\varepsilon=2M\sigma^2 t_f \tag{18}$$

Then, the stopping criterion is given by Eq. (16) with ε determined from Eq. (18).

5. Computational procedure

The computational procedure for the solution of this inverse problem using steepest descent method may be summarized as follows:

Suppose $h^n(S_i,t)$ is available at iteration n.

Step 1. Solve the direct problem given by Eq. (2) for $T(\Omega,t)$.
Step 2. Examine the stopping criterion given by Eq. (16) with ε given by Eq. (18). Continue if not satisfied.
Step 3. Solve the adjoint problem given by Eq. (12) for $\lambda(\Omega,t)$.
Step 4. Compute the gradient of the functional J' from Eq. (15).
Step 5. Compute the direction of descent P^n from Eq. (5).
Step 6. Set $\Delta h = P^n$, and solve the sensitivity problem given by Eq. (6) for $\Delta T(\Omega,t)$.
Step 7. Compute the search step size β^n from Eq. (9).
Step 8. Compute the new estimation for h^{n+1} from Eq. (4) and return to step 1.

6. Results and discussion

The objective of this study is to show the validity of the SDM in estimating the time-dependent local surface heat transfer coefficients for a 3-D plate finned-tube heat exchangers with no prior information on the functional form of the unknown function. The physical model for this problem is described as follows: The thermal conductivity for plate fin is taken as $k = 20$ W/(m K), $\rho = 7850$ kg/m^3, $Cp = 440$ J/(kg K); ambient temperature is chosen as $T_\infty = 296$ K and the temperatures on all tube surfaces are assumed as $T(S_i,t) = 353$ K, $i = 7$ to $(I + 6)$.

To illustrate the ability of the SDM in predicting $h(S_i,t)$, $i = 5$ and 6, with inverse analysis from the knowledge of the simulated measured temperature distributions on fin surface, we consider two numerical test cases with different variations of $h(S_i,t)$.

One of the advantages of using the SDM is that the initial guesses of the unknown heat transfer coefficients $h(S_i,t)$ can be chosen arbitrarily. In all the test cases considered here, the initial guesses for heat transfer coefficients used to begin the iteration are taken as $h(S_i,t) = 0.0$.

In order to compare the results for situations involving random measurement errors, we assume normally distributed uncorrelated errors with zero mean and constant standard deviation. The simulated inexact measurement data Y can be expressed as

$$Y_m = Y_{m,\text{exact}} + \omega\sigma \tag{19}$$

where $Y_{m,\text{exact}}$ is the solution of the direct problem with an exact heat transfer coefficients; σ is the standard deviation of the measurements; and ω is a random variable that generated by subroutine DRNNOR of the IMSL [13], ω is within -2.576 to 2.576 for a 99% confidence bound. In order to simplify the problem, the measurement errors on surface S_5 and S_6 are assumed the same.

We now present below two numerical experiments in determining $h(S_i,t)$ by the inverse analysis:

6.1. Numerical test case 1

The geometry and grid system for the first test case, i.e. staggered tube arrangement for a fin plate, are shown in Figs. 2a and 3a, respectively. The dimension for fin in x, y and z directions is 220 mm, 170 mm and 1 mm, respectively. The radius of tube is taken as 12.7 mm and the

longitudinal pitch of tube (i.e. the distance between center of two tubes) is 60.7 mm. The number of grid in z-direction is taken as 5 and the total grid number on x–y plane is 1456. The measured temperature extracting locations are at the grid points. The measurement time period Δt is 150 s and total measurement time t_f is 3750 s, i.e. there are 25 time steps. Therefore there exist totally of 36,400 unknown discrete heat transfer coefficients in this study.

The simulated exact function of the surface heat transfer coefficients on surfaces S_5 and S_6 in this numerical experiment is assigned in the following manner: (a). Firstly, solve Eq. (1a) by assuming the following boundary and initial conditions

$$T(S_3,t) = 20 + \frac{(y_{\max} - y)}{y_{\max}} \times 69 \quad \text{on } S_3, \text{ where } y_{\max} = 220 \tag{20a}$$

$$T(S_4,t) = 20 \quad \text{on } S_4 \tag{20b}$$

$$\frac{\partial T(S_i,t)}{\partial n} = 0 \quad \text{for the rest surfaces} \tag{20c}$$

$$T(S_i,0) = 20 \quad \text{at } t = 0 \tag{20d}$$

(b) Secondly, the values of the calculated temperature distributions on S_5 and S_6 are then taken as the simulated exact heat transfer coefficients for use in test case 1.

The three-dimensional inverse problem is first examined by using exact measurements, i.e. $\sigma = 0.0$. By setting stopping criteria $\varepsilon = 1.6 \times 10^6$, after 30 iterations the inverse solutions converged. The exact and estimated (or calculated) heat transfer coefficients $h(S_5,t)$ at time $t = 2250$ s and 3600 s are reported in Figs. 4 and 5, respectively.

The estimated heat transfer coefficients are also close to the exact values. The relative error between exact and estimated heat transfer coefficients is calculated as ERR1 = 2.92%, where ERR1 is defined as

$$\text{ERR1 } \% = \left[\sum_{j=1}^{J} \sum_{m=1}^{M} \left| \frac{h_m(S_5,j) - \hat{h}_m(S_5,j)}{h_m(S_5,j)} \right| \right] / (M \times J) \times 100\% \tag{21}$$

here J represents the index of discreted time, M indicates the number of grids and $\hat{h}_{m,j}(S_5)$ indicate the estimated values.

The corresponding measured and estimated temperature distributions at time $t = 2250$ s and 3600 s are shown in Figs. 6 and 7, respectively. By comparing Figs. 6 and 7 we find that the estimated temperatures are almost identical to the measured temperatures since the relative error between the measured and calculated temperatures is calculated as ERR2 = 0.025%, where ERR2 is defined as

$$\text{ERR2 } \% = \left[\sum_{j=1}^{J} \sum_{m=1}^{M} \left| \frac{T_m(S_5,j) - Y_m(S_5,j)}{Y_m(S_5,j)} \right| \right] / (M \times J) \times 100\% \tag{22}$$

here J represents the index of discreted time and M indicates the number of grids.

The inverse calculation is then proceed to consider the inexact temperature measurements. The standard deviation of the measurements is first taken as $\sigma = 0.1$, then it was increased to $\sigma = 0.3$.

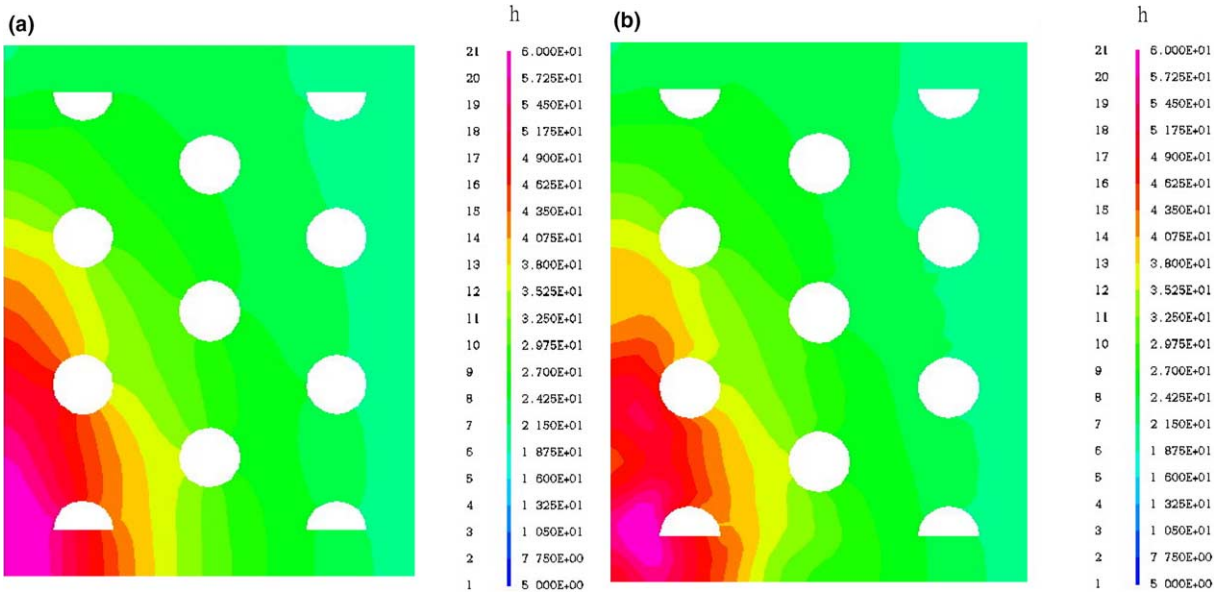

Fig. 4. The plots for (a) exact and (b) estimated heat transfer coefficients at $t = 2250$ s in test case 1 with $\sigma = 0.0$.

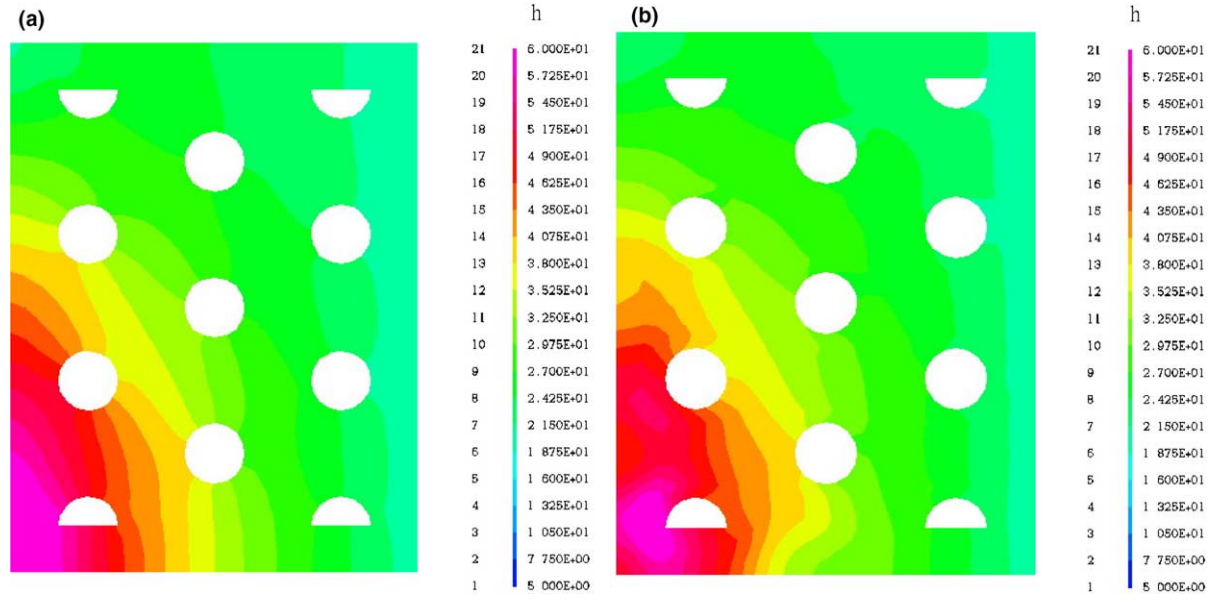

Fig. 5. The plots for (a) exact and (b) estimated heat transfer coefficients at $t = 3600$ s in test case 1 with $\sigma = 0.0$.

For $\sigma = 0.1$, 10 iterations are needed to satisfy the stopping criteria based on the discrepancy principle, the estimated heat transfer coefficients at time = 2250 s and 3600 s are shown in Fig. 8. The relative errors for heat transfer coefficients and temperatures are calculated as

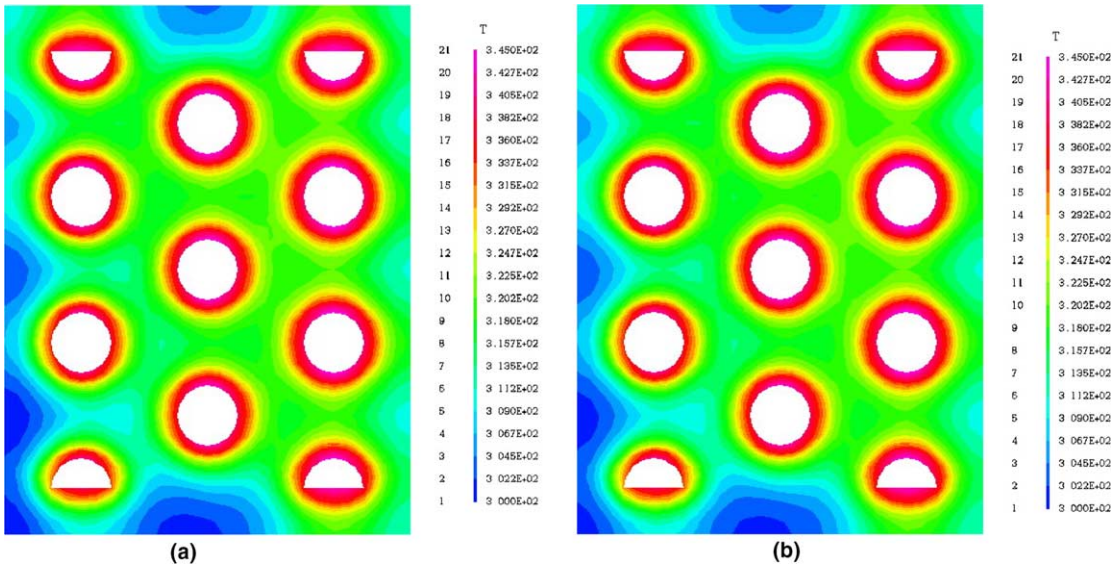

Fig. 6. The plots for (a) measured and (b) estimated temperatures at $t = 2250$ s in test case 1 with $\sigma = 0.0$.

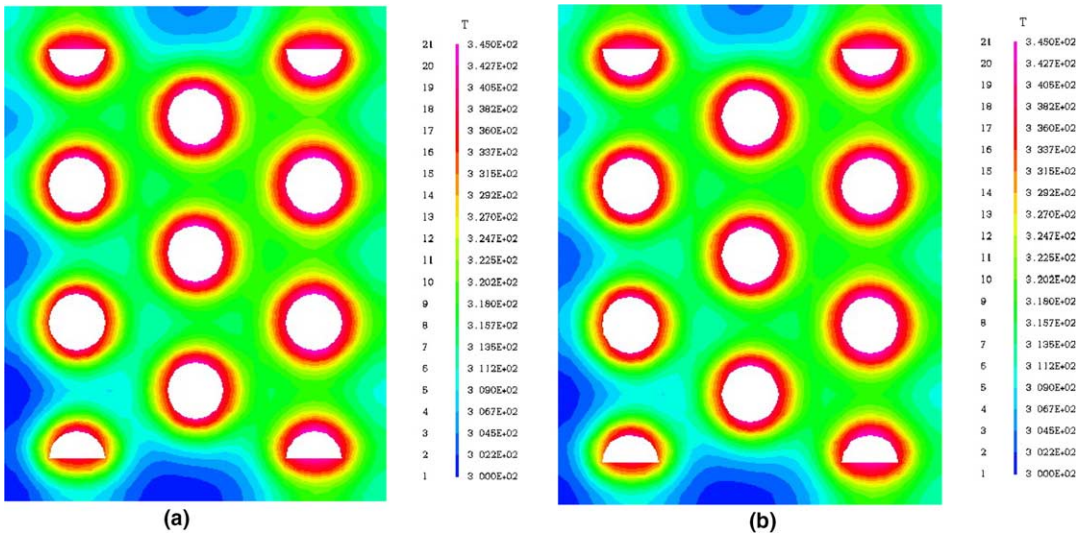

Fig. 7. The plots for (a) measured and (b) estimated temperatures at $t = 3600$ s in test case 1 with $\sigma = 0.0$.

ERR1 = 7.80% and ERR2 = 0.036%. For $\sigma = 0.3$, the number of iterations to satisfy the stopping criteria is only 8, the estimated heat transfer coefficients at time $t = 2250$ s and 3600 s are shown in Fig. 9, and the relative errors for heat transfer coefficients and temperatures are calculated as ERR1 = 11.6% and ERR2 = 0.068%.

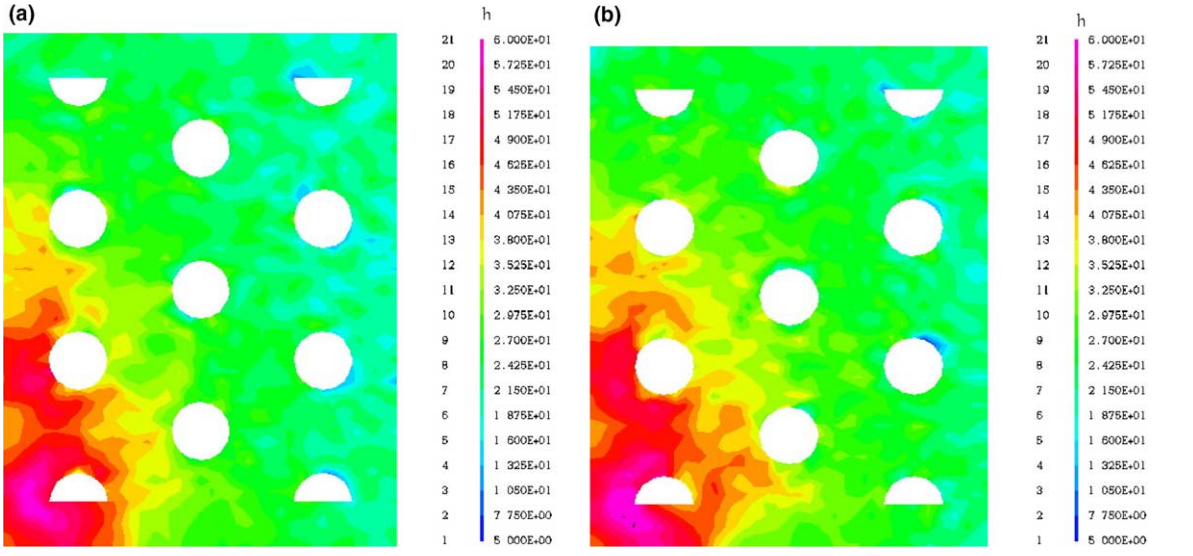

Fig. 8. The plots for the estimated heat transfer coefficients at (a) $t = 2250$ s and (b) $t = 3600$ s in test case 1 with $\sigma = 0.1$.

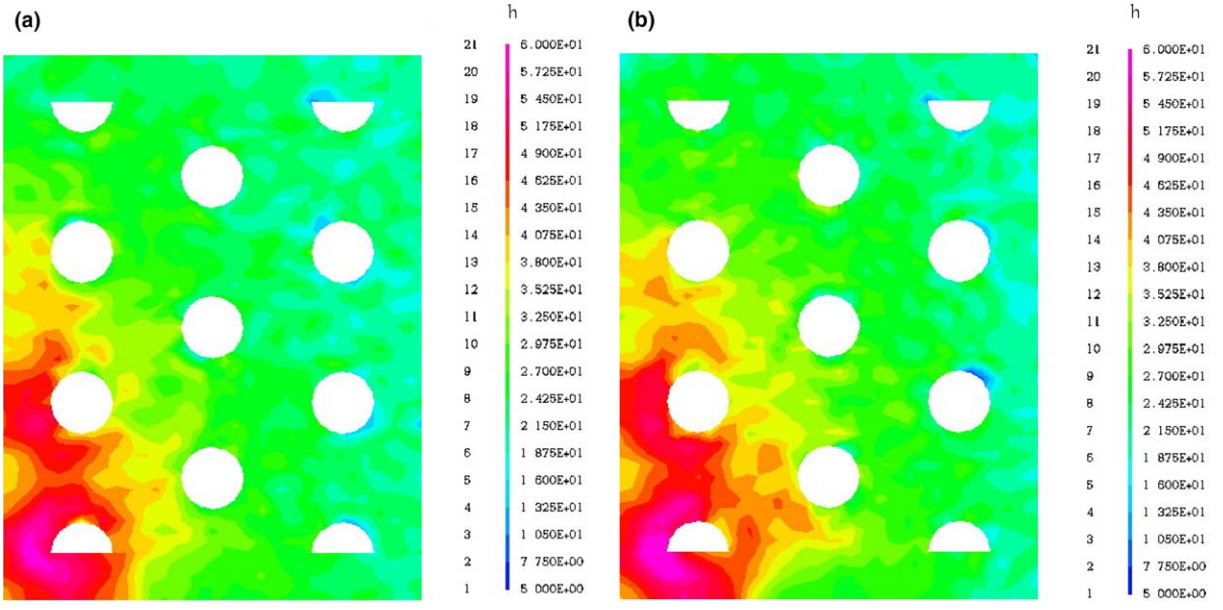

Fig. 9. The plots for the estimated heat transfer coefficients at (a) $t = 2250$ s and (b) $t = 3600$ s in test case 1 with $\sigma = 0.3$.

Based on above numerical results we learned that the estimated heat transfer coefficients are sensitive to the measurement errors, for this reason an accurate measurement technique is required for such kind of problem.

6.2. Numerical test case 2

In order to show the potential of the present algorithm for use in a transient three-dimensional inverse problem, we consider the second numerical test case. The geometry and grid systems for the second test case, i.e. in-line tube arrangement for a fin plate, are shown in Figs. 2b and 3b, respectively. The dimension for fin in x, y and z directions is 167 mm, 167 mm and 1 mm, respectively. The radius of tube is taken as 12.7 mm and the longitudinal pitch of tube (i.e. the distance between center of two tubes) is 60.7 mm. The number of grid in z-direction is taken as 5 and the total grid number on x–y plane is 1800. The measurement time period, total measurement time and thermal properties are taken the same as in case 1. Therefore there are totally of 45,000 unknown discrete heat transfer coefficients grids in this test case.

The exact function of the surface heat transfer coefficients on surfaces S_5 and S_6 in this numerical experiment is obtained in the following manner:

(a) Firstly, solve Eq. (1a) by assuming the following boundary and initial conditions

$$T(S_3, t) = 70 \quad \text{on } S_3 \tag{23a}$$

$$T(S_4, t) = 20 \quad \text{on } S_4 \tag{23b}$$

$$\frac{\partial T(S_i, t)}{\partial n} = 0 \quad \text{for the rest surfaces} \tag{23c}$$

$$T(S_i, 0) = 20 \quad \text{at } t = 0 \tag{23d}$$

(b) Secondly, the values of the calculated temperature distributions on S_5 and S_6 are then regarded as the exact heat transfer coefficients for use in test case 2.

When assuming $\sigma = 0.0$ and setting $\varepsilon = 2.4 \times 10^6$, after 30 iterations the estimated heat transfer coefficients can be obtained. The exact and estimated (or calculated) heat transfer coefficients

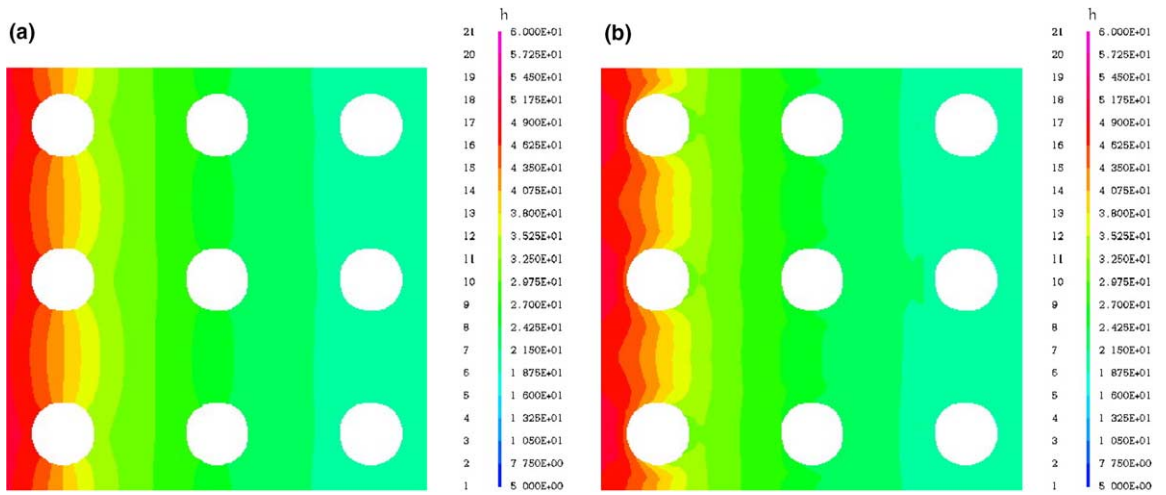

Fig. 10. The plots for (a) exact and (b) estimated heat transfer coefficients at $t = 2250$ s in test case 2 with $\sigma = 0.0$.

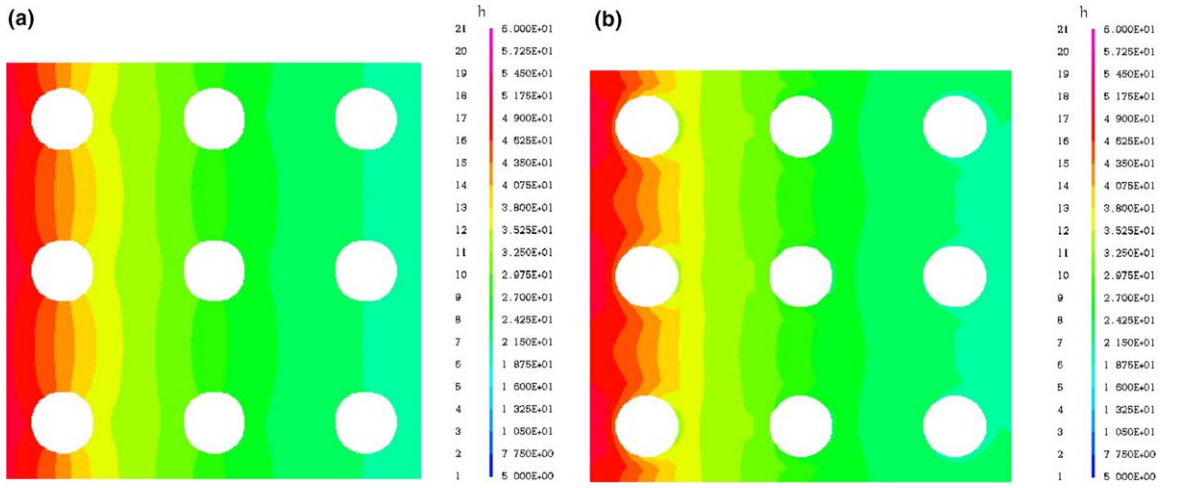

Fig. 11. The plots for (a) exact and (b) estimated heat transfer coefficients at $t = 3600$ s in test case 2 with $\sigma = 0.0$.

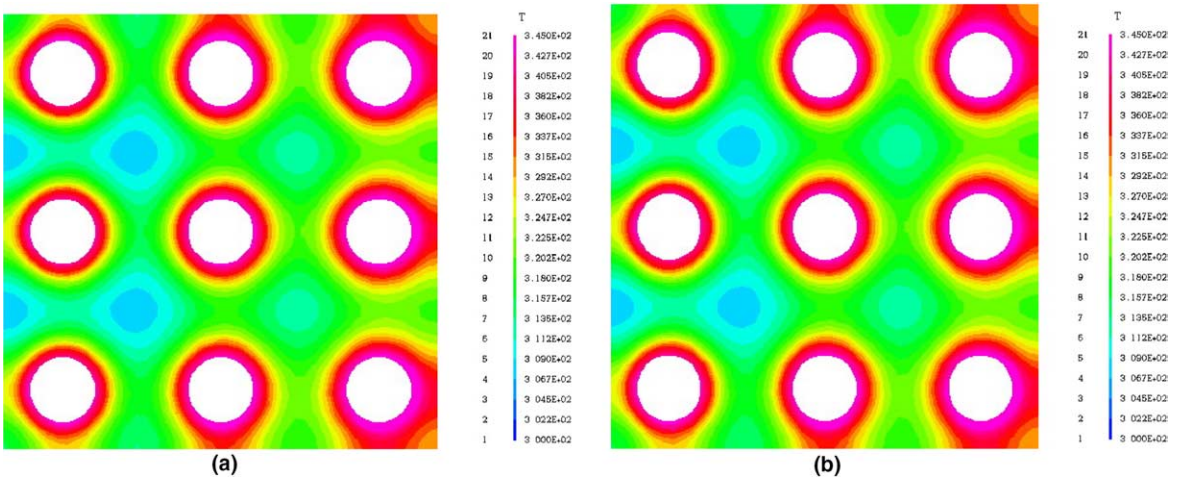

Fig. 12. The plots for (a) measured and (b) estimated temperatures at $t = 2250$ s in test case 2 with $\sigma = 0.0$.

$h(S_5, t)$ at time $t = 2250$ s and 3600 s are reported in Figs. 10 and 11, respectively. The measured and estimated temperature distributions at time $t = 2250$ s are shown in Fig. 12. ERR1 and ERR2 are calculated as 2.12% and 0.012%, respectively. The accuracy of the present algorithm is thus ensured.

Next, the inverse calculation is examined when the inexact temperature measurements are considered. The standard deviation of the measurements is taken as $\sigma = 0.3$. Seven iterations are needed to satisfy the stopping criteria based on the discrepancy principle, the estimated heat transfer coefficients at time $t = 2250$ s are shown in Fig. 13. The relative errors for heat transfer coefficients and temperatures are calculated as ERR1 = 12.3% and ERR2 = 0.057%, respectively.

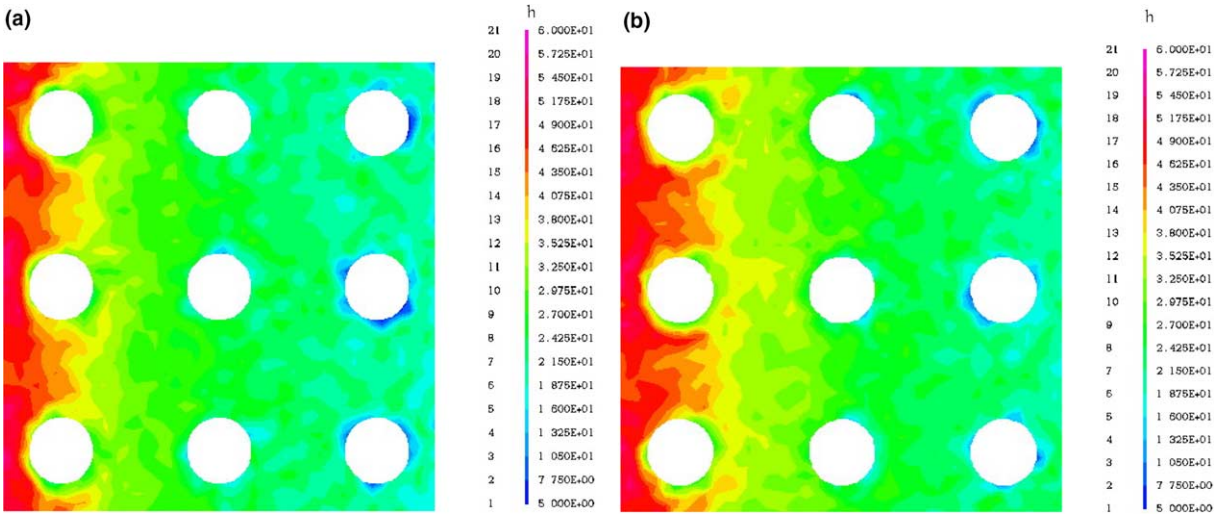

Fig. 13. The plots for the estimated heat transfer coefficients at (a) $t = 2250$ s and (b) $t = 3600$ s in test case 2 with $\sigma = 0.3$.

From above two numerical test cases we concluded that the SDM is now applied successfully in this 3-D inverse heat conduction problem for predicting the time-dependent surface heat transfer coefficients of plate fins.

7. Conclusions

The SDM with adjoint equation was successfully applied in determining the time-dependent local heat transfer coefficients for plate finned-tube heat exchangers for a 3-D inverse heat conduction problem. Two test cases involving different arrangement for fins, different type of heat transfer coefficients and different measurement errors were considered. The results show that the SDM does not require a priori information for the functional form of the unknown functions and the reliable estimated values can always be obtained.

Acknowledgement

This work was supported in part through the National Science Council, R.O.C., grant number, NSC-92-2611-E-006-007.

References

[1] W.M. Kays, A.L. London, Compact Heat Exchangers, third ed., Mcgraw-Hill, New York, 1984.
[2] H. Ay, J.Y. Jang, J.N. Yeh, Local heat transfer measurements of plate finned-tube heat exchangers by infrared thermography, Int. J. Heat Mass Transfer 45 (2002) 4069–4078.

[3] C.H. Huang, I.C. Yuan, H. Ay, A three-dimensional inverse problem in imaging the local heat transfer coefficients for plate finned-tube heat exchangers, Int. J. Heat Mass Transfer 46 (19) (2003) 3629–3638.
[4] CFX-4.4 User's Manual, AEA Technology Plc, Oxfordshire, UK, 2001.
[5] C.H. Huang, S.P. Wang, A three-dimensional inverse heat conduction problem in estimating surface heat flux by conjugate gradient method, Int. J. Heat Mass Transfer 42 (18) (1999) 3387–3403.
[6] C.H. Huang, W.C. Chen, A three-dimensional inverse forced convection problem in estimating surface heat flux by conjugate gradient method, Int. J. Heat Mass Transfer 43 (17) (2000) 3171–3181.
[7] C.H. Huang, S.C. Cheng, A three-dimensional inverse problem of estimating the volumetric heat generation for a composite material, Numer. Heat Transfer, Part A 39 (2001) 383–403.
[8] C.H. Huang, C.Y. Li, A three-dimensional optimal control problem in determining the boundary control heat fluxes, Heat Mass Transfer 39 (7) (2003) 589–598.
[9] T. Loulou, E.A. Artioukhine, Optimal choice of descent steps in gradient-type methods when applied to combined parameter and function or multi-function estimation, Inverse Prob. Eng. 11 (2003) 273–288.
[10] H. Louahlia-Gualous, P.K. Panday, E.A. Artioukhine, Inverse determination of the local heat transfer coefficients for nucleate boiling on a horizontal cylinder, J. Heat Transfer—Trans. ASME 125 (2003) 1087–1095.
[11] T. Loulou, E.P. Scott, Estimation of 3-dimensional heat flux from surface temperature measurements using an iterative regularization method, Heat Mass Transfer 39 (2003) 435–443.
[12] O.M. Alifanov, Inverse Heat Transfer Problem, Springer-Verlag, Berlin, 1994.
[13] IMSL Library Edition 10.0, User's Manual: Math Library Version 1.0, IMSL, Houston, TX, 1987.